

## TARGET DETECTION IN PULSE-TRAIN MIMO RADARS APPLYING ICA ALGORITHMS

M. Hatam<sup>\*</sup>, A. Sheikhi, and M. A. Masnadi-Shirazi

Department of Electrical Engineering and Computer Science, Shiraz University, Shiraz, Iran

**Abstract**—In this paper, the problem of target detection in co-located “multi-input multi-output” (MIMO) radars is considered. A pulse-train signaling is assumed to be used in this system. As the doppler effect should be considered for the pulse-train signaling, we are confronted by a compound hypothesis testing problem, so in this paper a Generalized Likelihood Ratio (GLR) detector is derived. The high complexity of this detector makes us derive a new detector based on the theory of Independent Component Analysis (ICA). It is shown that the computational load of the ICA-based detector is much less than the GLR detector. It is also shown that the sensitivity of the ICA-based detector to the doppler effect is very low. According to this approach, an appropriate signal design method is presented, based on the separation performance of the ICA algorithms. It is shown that independent random sequences are proper signals in the sense of detection performance.

### 1. INTRODUCTION

The development of phased array radars has enabled designers to improve estimation and detection performance of radar systems [1, 2]. The ability to exploit these improvements is limited by the realizable number of receiver elements. Recently, researchers tend to develop a new radar structure known as multiple-input multiple-output (MIMO) radar [3–16]. In the concept of MIMO radars, multiple antennas are used to transmit several waveforms and employed to receive the echoes reflected by the targets.

The two major types of MIMO radars are “widely separated” and “co-located” MIMO radars. In the first type, in order to use spatial

---

*Received 12 October 2011, Accepted 30 November 2011, Scheduled 5 December 2011*

<sup>\*</sup> Corresponding author: Majid Hatam (hatammajid@gmail.com).

diversity of target reflection, the distances between antenna elements are very large compared to the signal wavelength [4]. The diversity of Radar Cross Section (RCS) improves the detection performance in this type [12]. Different works are presented in signaling and target detection of widely separated MIMO radars [13, 17, 18].

Co-located MIMO radar structure is a widespread type of MIMO radars that is quite similar to the phased-array radars [8]. In this type, for a given number of receiver elements, signal diversity can virtually increase the effective number of array elements. In other words, the signal diversity leads to an increase in the virtual aperture of receiving array [8]. In the co-located MIMO radars, a point target model is usually assumed, and also far-field signal source and narrow-band transmitted signal are considered. Co-located MIMO radars have many advantages compared to the traditional approach of phased array signaling. Improvement of angle estimation, better angular Side-Lobe Level (SLL) and beam shape characteristics are some of these advantages [8, 19, 20].

These benefits can be obtained only with the assumption of ideal signal separation in the receiver. In other words, orthogonality should be considered for the transmitted signals [10]. But for MIMO radars with numerous transmit elements, it is very difficult to find fully orthogonal signals. Only frequency separated signals are offered as fully orthogonal signals for MIMO radar signaling [21–23].

Another signaling approach is to transmit  $m$  orthogonal base-band signals or codes on a single carrier frequency. In this signaling, a bank of matched-filters or correlators is used to separate these signals in each receiver [10, 24]. There are some problems in this approach that cannot be neglected. Range side-lobe level is the first problem that destroys the radar resolution capability when strong and weak targets are near each other. The most important problem is to find a set of orthogonal signals to fulfill all radar signaling restrictions. Even if it is possible to find orthogonal signals, the doppler effect will destroy the orthogonality [25]. Few works on target detection in co-located MIMO radars, are all based on this type of signaling. Presenting a new space-time coding configuration for target detection and localization is an example [10]. The ability to steer the transmitted beam pattern had been the main advantage of this research. The second example is designing detectors for non-Gaussian clutter condition [26].

In [25], a pulse-train signaling for co-located MIMO radars has been proposed. In the former techniques, an inter-pulse code modulation has been employed (first row of Fig. 1). But in the proposed technique, a pulse-train signaling approach is utilized, and an intra-pulse code modulation is employed (second row of Fig. 1). In

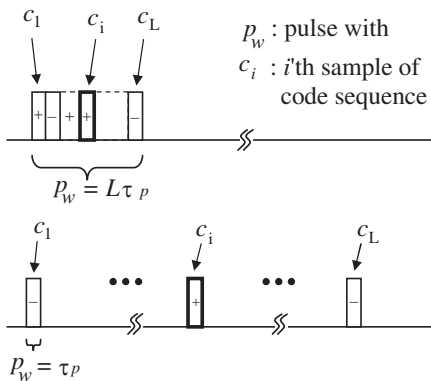


**Figure 1.** Comparison of the inter-pulse and the intra-pulse code modulations.

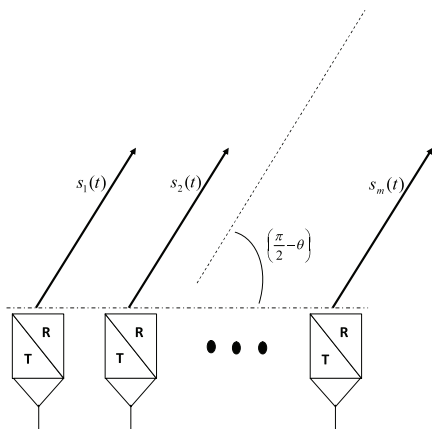


**Figure 2.** A uniform linear array by a set of  $m$  jointly transmitter/receiver antenna elements.

this approach, each radar transmitting element radiates a unique batch of pulses coded in phase and/or amplitude.

In the presented signaling, different carrier frequencies are used in different transmitters. Applying the frequency difference of  $\Delta f = 1/\tau_p$  to all  $m$  transmitters, the range resolution can be improved to  $c\tau_p/2m$  according to the idea of “Stepped Frequency Radars” [27–29]. In the inter-pulse modulation signaling, the codes should be designed according to the criteria of good separability and proper pulse compression property. But in the proposed signaling the codes should be designed only based on the separability criterion and the pulse compression is achieved by the stepped frequency idea. So, the complexity of code design is decreased in the proposed signaling scheme.

In this paper, the problem of target detection in MIMO radars using this type of signaling is considered. The received signal modeling and problem formulation are presented in Section 2. It is shown that due to unknown values of doppler frequency and target DOA, a compound hypothesis testing problem is confronted. The standard technique for compound hypothesis tests when the Probability Distribution Function (PDF) of the unknown parameters are not known is the Generalized Likelihood Ratio (GLR) detection.

In Section 3, the GLR detector is derived. Except invariance and asymptotic performance, there is no optimality claimed on GLR [30]. So, it is reasonable to investigate other detection strategies.

In Section 4, the problem formulation is simplified and applying Independent Component Analysis (ICA) algorithms, an ICA-based detector is presented. A brief review on ICA techniques is also offered in this section. To achieve a good detection performance, the performance of ICA techniques for separation of different transmitted signals is considered as a constraint to design a set of codes for pulse-train signaling. This signal design technique is presented in Section 5. A brief analysis of computational complexity of two presented detectors is offered in Section 6. Finally, in Section 7 simulation results are presented to evaluate the detection performance of the proposed detectors.

## 2. PROBLEM FORMULATION

Without loss of generality, in this paper a co-located MIMO radar with a Uniform Linear Array (ULA) is considered which is formed by a set of  $m$  jointly transmitting/receiving antenna elements separated by  $0.5\lambda$  (Fig. 2).<sup>†</sup> The pulse-train signaling proposed in [25] is used. Considering a fixed pulse width of  $\tau_p$  and the Pulse Repetition Interval (PRI) of  $T_p$ , the narrow-band transmitted pulse trains are denoted by  $s_k(t)$ ,  $k = 1, \dots, m$ :

$$\begin{cases} s_k(t) \neq 0 & q \times T_p \leq t \leq q \times T_p + \tau_p \\ s_k(t) = 0 & \text{else} \end{cases} \quad (1)$$

where  $q = 0, 1, 2, \dots, L$  and  $L$  is the number of transmitted pulses from each transmitter. In this signaling, a single chip pulse with suitable duration  $\tau_p$ , according to the desired range resolution ( $c\tau_p/2m$ ) is transmitted during each  $T_p$ . In each transmitted pulse train, the amplitude and phase of signal can be changed in a suitable manner to make all  $s_k(t)$ s separable. It is assumed that the transmitted signals have different carrier frequencies, with  $\Delta f = 1/\tau_p$  differences. If the center carrier frequency is denoted by  $f_c$ , each transmitted signal has a small frequency shift of  $\Delta f_k = (k - \frac{m+1}{2}) \times \Delta f$  related to  $f_c$ . So the  $m \times 1$  vector of base-band received signal from a far-filled point target, for each transmitted signal is given by:

$$\mathbf{x}_k(t) = \alpha \mathbf{e}_k(\theta) b_k(\theta) s_k(t - \tau) \exp(2\pi i (f_{d_k} + \Delta f_k) t + i \times k\phi) \quad (2)$$

where  $\tau$  is the received signal delay and  $\phi = -2\pi\Delta f \times \tau$  is the phase related to this delay.  $\alpha$  is a complex constant, containing the effect

<sup>†</sup> Here, we assume an equal number of transmitting and receiving elements. In our model, it is possible to have different numbers of them. But the number of receiving elements should be more than or at least equal to the number of transmitting elements.

of power, RCS and propagation loss. For a single point target in this model,  $\alpha$  is constant for all the transmitted signals, due to the co-located antenna assumption.  $\mathbf{e}(\theta)$  is the  $m \times 1$  array factor of receiving antennas for the direction of target,  $b_k(\theta)$  is the  $k$ th transmitter factor and depends on the direction of target and  $f_{d_k}$  is the target doppler frequency. Assuming radial velocity  $V$ ,  $f_{d_k}$  is given by:

$$f_{d_k} = \frac{2V}{\lambda_k} = \frac{2V}{\lambda} \times \frac{\lambda}{\lambda_k} = f_d \times \frac{\lambda}{\lambda_k} \tag{3}$$

where  $\lambda_k$  is the wavelength of  $k$ th transmitted signal and  $f_d$  is the doppler value, corresponding to  $\lambda$  that is the center wavelength. Completely similar to the theory of ‘‘Stepped Frequency Radars’’ [27, 28], the range dependent phase variation can be used to improve the range resolution of this system. If we set  $\Delta f = 1/\tau_p$ , and if the delay is  $\tau = n \times \tau_p + \delta_\tau$ , the phase would be  $\phi = -2\pi n - 2\pi \frac{\delta_\tau}{\tau_p} = -2\pi \frac{\delta_\tau}{\tau_p}$ . As we have only  $m$  samples to estimate  $\phi$ , the resolution of phase estimation is about  $2\pi/m$  that is identical to the range resolution of  $c\tau_p/2m$ .

We define  $f_k = (f_{d_k} + \Delta f_k)$  for each transmitted signal and so we can rewrite (2) as:

$$\mathbf{x}_k(t) = \alpha \mathbf{e}_k(\theta) b_k(\theta) s_k(t - \tau) \exp(2\pi i f_k t + i \times k\phi) \tag{4}$$

The  $j$ th element of  $\mathbf{e}_k(\theta)$  is given by:

$$\{\mathbf{e}_k(\theta)\}_j = \exp\left\{2\pi i \frac{d_j}{\lambda_k} \sin(\theta)\right\} \quad j, k = 1, \dots, m \tag{5}$$

Here,  $d_j$  indicates the relative position of the  $j$ th receiving element from the array center. Also, we can formulate the  $k$ th transmitter factor  $b_k(\theta)$  as:

$$b_k(\theta) = \exp\left\{2\pi i \frac{d_k}{\lambda_k} \sin(\theta)\right\} \quad k = 1, \dots, m \tag{6}$$

Considering  $\mathbf{n}(t)$  as the vector of additive Gaussian noise of receiver elements, the vector of received signal ( $\mathbf{x}(t)$ ), would be:

$$\begin{aligned} \mathbf{x}(t) &= \sum_{k=1}^m \mathbf{x}_k(t) + \mathbf{n}(t) \\ &= \sum_{k=1}^m \alpha \mathbf{e}_k(\theta) b_k(\theta) \exp(i \times k\phi) s_k(t - \tau) \exp(2\pi i f_k t) + \mathbf{n}(t) \\ &= \alpha \sum_{k=1}^m \mathbf{a}_k(\theta, \phi) \tilde{s}_k(t - \tau) + \mathbf{n}(t) = \alpha \mathbf{A}(\theta, \phi) \tilde{\mathbf{S}}(t - \tau) + \mathbf{n}(t) \end{aligned} \tag{7}$$

where the  $m \times 1$  vector  $\mathbf{a}_k(\theta, \phi)$  which is the  $k$ th column of the  $m \times m$  mixing matrix  $\mathbf{A}(\theta, \phi)$ , is given by:

$$\{\mathbf{a}_k(\theta, \phi)\}_j = \{\mathbf{e}_k(\theta)\}_j b_k(\theta) \exp(i \times k\phi) \quad j = 1, \dots, m \quad (8)$$

$\tilde{\mathbf{s}}(t - \tau)$  is the  $m \times 1$  vector of delayed and frequency shifted source signals and we have:

$$\{\tilde{\mathbf{s}}(t - \tau)\}_k = \mathbf{s}_k(t - \tau) \exp(2\pi i f_k t) \quad k = 1, \dots, m \quad (9)$$

In this model, the direction of target ( $\theta$ ), the exact value of  $\phi$  and the doppler value of signal ( $f_d$ ) are assumed to be unknown. Considering the pulse repetition interval of  $T_p$ , after range sampling of the received array signal at times  $t = \ell \times T_p + r\tau_p$  for  $\ell = 1, \dots, L$  and  $r = 1, \dots, \frac{T_p}{\tau_p}$ , we have  $R = \frac{T_p}{\tau_p}$  range cells and we can form a  $m \times L$  matrix of received data for each range cell in which  $L$  denotes the number of transmitted/received pulses. If  $\tau = n \times \tau_p + \delta_\tau$ , for the  $n$ th range cell, we have:

$$\mathbf{X}_{m \times L} = \alpha \mathbf{A}(\theta, \phi) \tilde{\mathbf{S}}_{m \times L} + \mathbf{N}_{m \times L} = \alpha \sum_{k=1}^m \mathbf{a}_k(\theta, \phi) \tilde{\mathbf{s}}_k^T + \mathbf{N}_{m \times L} \quad (10)$$

where  $\mathbf{N}$  contains the independent samples of receiver Gaussian noise. In this notation,  $(.)^T$  denotes transpose and the  $L \times 1$  vector  $\tilde{\mathbf{s}}_k$  which is the  $k$ th column of  $\tilde{\mathbf{S}}_{m \times L}$ , contains the samples of  $\tilde{s}_k(t - \tau)$  at the desired delay for  $L$  consecutive pulses. Each element of  $\tilde{\mathbf{s}}_k$  can be written as:

$$\{\tilde{\mathbf{s}}_k\}_\ell = \{\mathbf{s}_k\}_\ell \times \exp(2\pi i f_k (\ell \times T_p + n\tau_p)) \quad (11)$$

where  $\{\mathbf{s}_k\}_\ell = s_k(\ell \times T_p + \delta_\tau)$ . Now, we can form the detection problem as:

$$\begin{aligned} \mathbf{X} &= \alpha \mathbf{A}(\theta, \phi) \tilde{\mathbf{S}}(f_d) + \mathbf{N} & (12) \\ \begin{cases} H_0 : & \alpha = 0 \\ H_1 : & \alpha \neq 0 \end{cases} \end{aligned}$$

where  $\theta$ ,  $f_d$ ,  $\phi$  and  $\alpha$  are unknown parameters and so (12) is a compound hypothesis testing problem. In this paper, we assume that all of the receiver noise vectors are  $\mathcal{N}(0, \sigma_n^2 \mathbf{I}_m)$  where  $\sigma_n^2$  is known and the noise vectors of different receiver elements are independent.

When the PDFs of the unknown parameters are not known and the Uniformly Most Powerful (UMP) detectors can not be found, the standard technique for compound hypothesis tests would be the GLR detector. There is no optimality claimed about GLR, except invariance and asymptotic performance [30]. So, it is reasonable to investigate other detection strategies. In the next sections, different detectors for this problem would be proposed.

### 3. GLR DETECTOR

The GLR detector for the compound hypothesis test of (12) is:

$$\frac{f_X \left( X|H_1, \hat{\theta}, \hat{\alpha}, \hat{\phi}, \hat{f}_d \right)}{f_X \left( X|H_0 \right)} \geq \eta \tag{13}$$

where  $\hat{\theta}$ ,  $\hat{\alpha}$ ,  $\hat{\phi}$  and  $\hat{f}_d$  are the Maximum Likelihood (ML) estimations of  $\theta$ ,  $\alpha$ ,  $\phi$  and  $f_d$ , respectively. This GLR detector is derived for the compound hypothesis test of (12) in Appendix A and is given by:

$$\max_{f_d, \theta, \phi} \frac{\left| \text{tr} \left( \mathbf{A}(\theta, \phi) \tilde{\mathbf{S}}(f_d) \mathbf{X}^H \right) \right|^2}{\left\| \mathbf{A}(\theta, \phi) \tilde{\mathbf{S}}(f_d) \right\|^2} \geq \eta \tag{14}$$

In this notation,  $\text{tr}(\cdot)$  denotes trace of matrix. It is determined that the GLR detector leads to a maximization over all realizable values of  $\theta$ ,  $\phi$  and  $f_d$  and also comparing this maximum with a threshold. If  $n_f$  is the number of desired doppler values in the interval of  $[0, \text{PRF})$ ,  $n_\phi$  is the number of phase test points and  $n_\theta$  is the number of direction test points in the interval of  $[0, \pi]$ , the complexity of this detector can be justified with  $n_f \times n_\theta \times n_\phi$  that requires a heavy processing power. The frequency space of doppler test point and also, the space between direction test point are very important in this method. But increasing the number of doppler, phase and direction test points, would enhance the computational complexity of GLR detection algorithm.

In the next section, it will be shown that considering the statistical characteristics of transmitted pulse trains, the ML estimated parameters used in the GLR detector can be replaced by ICA estimated values of these parameters to form an ICA-based detector.

### 4. ICA-BASED DETECTOR

In pulse-train technique, we can change the amplitude and/or phase of signal in a certain manner for each transmitter unit. Random or pseudo-random pulse to pulse coding is a good example. The randomness and independency of transmitted signals from pulse to pulse, enable us to use ICA algorithms as a proper solution in estimation of unknown parameters. Therefore, instead of applying ML estimator in the structure of GLR detector, an ICA estimator can be applied. So, we present the ICA-based detector as:

$$\frac{f_X \left( X|H_1, \check{\theta}, \check{\alpha}, \check{\phi}, \check{f}_d \right)}{f_X \left( X|H_0 \right)} \geq \eta \tag{15}$$

where  $\check{\theta}$ ,  $\check{\alpha}$ ,  $\check{\phi}$  and  $\check{f}_d$  are the ICA estimations of  $\theta$ ,  $\alpha$ ,  $\phi$  and  $f_d$ . In Appendix B, it has been shown that the decisive rule of (15) is equivalent to:

$$\left| 2\text{Re} \left[ \text{tr} \left( \check{\alpha} \mathbf{A}(\check{\theta}, \check{\phi}) \check{\mathbf{S}}(\check{f}_d) \mathbf{X}^H \right) \right] - \left\| \check{\alpha} \mathbf{A}(\check{\theta}, \check{\phi}) \check{\mathbf{S}}(\check{f}_d) \right\|^2 \right| \geq \eta \quad (16)$$

It should be noted that instead of  $\check{\theta}$ ,  $\check{\alpha}$ ,  $\check{\phi}$  and  $\check{f}_d$ , we only need to estimate  $\check{\alpha} \mathbf{A}(\check{\theta}, \check{\phi})$  and  $\check{\mathbf{S}}(\check{f}_d)$ . Before presenting the complete solution of the ICA-based estimators, a brief review to ICA is offered in the next subsection.

#### 4.1. ICA Model

The theory of ICA, is totally described in [31–34]. In the standard ICA model, we suppose a linear structure of the form:

$$\mathcal{X} = \mathcal{A}\mathcal{S} + \mathcal{N} \quad (17)$$

when  $\mathcal{S}$  is an  $m \times L$  dimensional matrix of source signals. The rows of  $\mathcal{S}$ , named  $s_k^T$ ,  $k = 1, \dots, m$  are all independent and each  $s_k^T$  is a vector of  $L$  i.i.d samples.  $\mathcal{A}$  is the unknown  $m \times m$  mixture matrix and  $\mathcal{N}$  is the additive Gaussian noise. Also,  $\mathcal{X}$  is the available data matrix in which any row ( $x_k^T$ ) is a linear mixture of independent source signals ( $s_k^T$ ) contaminated with noise.

Different ICA methods are all designed to estimate  $\mathcal{A}$  or equivalently  $\mathcal{W} = \mathcal{A}^{-1}$  and the source signals,  $\mathcal{S}$ . Since  $\mathcal{A}$  and  $\mathcal{S}$  are both unknown, without assuming independent source signals, the problem cannot be solved in general. Different ICA methods use different available statistical properties of signals to solve this estimation problem. ICA finds the desired sources by maximizing the statistical independence of the estimated components. There are many ways to define independency and each way may result in a different form of the ICA algorithm. The two major definitions for independence in ICA are based on “Minimization of Mutual Information” and “Maximization of non-Gaussianity”.

The family of ICA algorithms, based on maximization of non-Gaussianity, originate from the idea of central limit theorem. Higher order statistics are proper tools to measure the non-Gaussianity of signals. JADE, introduced by Cardoso [35], is the most commonly used method in this class. Because of the proper performance for separation of complex signals, in this paper we focus on using the complex form of the JADE algorithm [36].

ICA methods have two common restrictions. The first is that they cannot determine the power and phase of source signals and the

second is that the separation is not possible for signals with Gaussian distribution. Due to the ambiguity in signal power, it would be better to assume that the variances of source signals are equal to one. Also, in most ICA methods, without loss of generality, it is assumed that both the data and source signals have a zero mean. In order to simplify the problem for the practical iterative algorithms, typical ICA methods use centering, whitening, and dimension reduction as their preprocessing steps [31].

One important property of ICA methods is that most of the criteria used as the base of these techniques are not influenced by additive Gaussian noise. For example, the higher order cumulants are not affected by the additive Gaussian signals. Therefore, theoretically JADE and other algorithms that are based on higher order cumulants, are immune to Gaussian noise for estimating the mixing matrix. But in practice, because of the limited number of samples, the approximate values of cumulants are affected by Gaussian noise, which would increase the error in estimating the mixing matrix. So, to decrease the noise effect, a noise reduction filter is usually applied before ICA estimation [31]. A Wiener filter is the ideal structure for noise cancelation in this case (Appendix C).

The “ICA estimated” signals usually have two ambiguities.

- 1) The proper scaling or phase of the source signals.
- 2) A uniquely correct ordering of the source signals.

Comparing Equations (17) and (12) shows that the MIMO radar problem can be considered as an ICA problem in which  $\mathcal{A} = \alpha \mathbf{A}(\theta, \phi)$ ,  $\mathcal{S} = \tilde{\mathbf{S}}(f_d)$  and  $\mathcal{N} = \mathbf{N}$ . So, the estimation of  $\alpha \mathbf{A}(\theta, \phi)$  and  $\tilde{\mathbf{S}}(f_d)$  can be derived using ICA techniques. In this problem, the two ambiguities mentioned above cannot be ignored and should be solved in the MIMO radar problem. So, as it will be described in the following section, a proper solution is proposed for removing these ambiguities.

#### 4.2. Derivation of ICA-based Detector

In the problem of pulse-train signaling with unknown values of  $f_d$  and  $\theta$ , we confront an ICA problem of the form demonstrated in Equation (10). Solving this complex ICA problem, we will find a linear estimator named  $\hat{\mathbf{W}}$  that ideally should be equal to  $(\alpha \mathbf{A})^{-1}$ . Also, the estimation of received signal is derived by applying  $\hat{\mathbf{W}}$  to the received signal as:

$$\hat{\mathbf{Y}} = \hat{\mathbf{W}}\mathbf{X} = \hat{\mathbf{W}}\alpha\mathbf{A}\tilde{\mathbf{S}} + \hat{\mathbf{W}}\mathbf{N} \quad (18)$$

Because of the nature of ICA techniques, even if we consider an ideal solution and a noise-free signal model, still there is an inevitable

ambiguity in the phase and order of signals that can be formulated as:

$$\hat{\mathbf{y}}_k = \exp(i\varphi_k) \times \tilde{\mathbf{s}}_j \quad \hat{\xi}_k = \exp(-i\varphi_k) \times \mathbf{a}_j \quad (19)$$

where the  $L \times 1$  vector  $\hat{\mathbf{y}}_k$  is the  $k$ th estimated signal ( $k$ th row of  $\hat{\mathbf{Y}}$ ) which does not normally correspond to the  $k$ th signal  $\hat{\mathbf{s}}_k$ . Also,  $\hat{\xi}_k$  is the  $k$ th column of  $\hat{\mathbf{W}}^{-1}$  which is not necessarily equal to the  $k$ th column of  $\alpha\mathbf{A}$  and  $\varphi_k$ s are arbitrary phases. Now, in order to complete the estimation process, these ambiguities should be removed.

#### 4.2.1. Arrangement and Phase Correction

We can rewrite (19) as

$$\hat{\mathbf{y}}_k = \mathbf{h}_j(f_d)\rho_k \quad (20)$$

where  $\rho_k = \exp(j\varphi_k)$ ,  $\mathbf{h}_j(f_d)$  is an  $L \times 1$  vector and  $[\mathbf{h}_j(f_d)]_\ell = [\tilde{\mathbf{s}}_j]_\ell = [\mathbf{s}_j]_\ell \times \exp\{2\pi i(f_d \cdot \frac{\lambda}{\lambda_j} + \Delta f_j)t_\ell\}$  where  $t_\ell = \ell \times T_p + n\tau_p$ . Then the Least-Squares (LS) estimator for the unknown parameters minimizes  $J$ , as shown below:

$$J(\rho_k, j, f_d) = (\hat{\mathbf{y}}_k - \mathbf{h}_j(f_d)\rho_k)^H(\hat{\mathbf{y}}_k - \mathbf{h}_j(f_d)\rho_k) \quad (21)$$

To solve this minimization problem, first we suppose that  $f_d$  and  $j$  or equivalently  $\mathbf{h}_j(f_d)$  are known, then we have:

$$\hat{\rho}_k = (\mathbf{h}_j^H(f_d)\mathbf{h}_j(f_d))^{-1}\mathbf{h}_j^H(f_d)\hat{\mathbf{y}}_k \quad (22)$$

replacing (22) in (21) we have

$$\begin{aligned} J(j, f_d) &= (\hat{\mathbf{y}}_k - \mathbf{h}_j(f_d)\left(\mathbf{h}_j^H(f_d)\mathbf{h}_j(f_d)\right)^{-1}\mathbf{h}_j^H(f_d)\hat{\mathbf{y}}_k)^H \\ &\quad \times (\hat{\mathbf{y}}_k - \mathbf{h}_j(f_d)\left(\mathbf{h}_j^H(f_d)\mathbf{h}_j(f_d)\right)^{-1}\mathbf{h}_j^H(f_d)\hat{\mathbf{y}}_k) \\ &= \hat{\mathbf{y}}_k^H \left( I - \mathbf{h}_j(f_d)\left(\mathbf{h}_j^H(f_d)\mathbf{h}_j(f_d)\right)^{-1}\mathbf{h}_j^H(f_d) \right) \hat{\mathbf{y}}_k \end{aligned} \quad (23)$$

since  $(I - \mathbf{h}^H\mathbf{h})^{-1}\mathbf{h}^H$  is an idempotent matrix [37], minimization of  $J(j, f_d)$  is equivalent to maximizing  $J'(j, f_d)$  as

$$J'(j, f_d) = \hat{\mathbf{y}}_k^H \mathbf{h}_j(f_d)\left(\mathbf{h}_j^H(f_d)\mathbf{h}_j(f_d)\right)^{-1}\mathbf{h}_j^H(f_d)\hat{\mathbf{y}}_k \quad (24)$$

then the estimator is given by:

$$\begin{aligned} (\hat{j}, \hat{f}_d^k) &= \arg \max_{j=1, \dots, m, f_d \in [0, \text{PRF}]} (J'(j, f_d)) \\ &= \arg \max_{j, f_d} \left( \frac{\left| \sum_{\ell=1}^n \hat{\mathbf{y}}_k[\ell] \mathbf{s}_j^*[\ell] \exp\left\{-2\pi i\left(f_d \cdot \frac{\lambda}{\lambda_j} + \Delta f_j\right) \cdot t_\ell\right\}\right|^2}{\sum_{\ell=1}^n \left| \mathbf{s}_j[\ell] \exp\left\{2\pi i\left(f_d \cdot \frac{\lambda}{\lambda_j} + \Delta f_j\right) \cdot t_\ell\right\}\right|^2} \right) \end{aligned} \quad (25)$$

Considering equal power for the transmitted signals, this estimator can be simplified as a windowed periodogram estimator as:

$$\begin{aligned}
 (\hat{j}, \hat{f}_d^k) &= \operatorname{argmax}_{j, f_d} (J'(j, f_d)) \\
 &= \operatorname{argmax}_{j, f_d} \left( \frac{1}{N} \left| \sum_{\ell=1}^n \hat{\mathbf{y}}_k[\ell] \mathbf{s}_j^*[\ell] \exp \left\{ -2\pi i \left( f_d \cdot \frac{\lambda}{\lambda_j} + \Delta f_j \right) \cdot t_\ell \right\} \right|^2 \right) \quad (26)
 \end{aligned}$$

Applying this estimator, the arrangement is complete. According to (25), (26), the arrangement of signals can be performed with a weighted FFT in practice. After signal arrangement, the estimated vector  $\mathbf{h}_{\hat{j}}(\hat{f}_d^k)$ , should be applied to (22). So the phase estimator is given by:

$$\hat{\rho}_k = \left( \mathbf{h}_{\hat{j}}(\hat{f}_d^k)^H \mathbf{h}_{\hat{j}}(\hat{f}_d^k) \right)^{-1} \mathbf{h}_{\hat{j}}(\hat{f}_d^k)^H \hat{\mathbf{y}}_k \quad (27)$$

where  $[\mathbf{h}_{\hat{j}}(\hat{f}_d^k)]_\ell = [\mathbf{s}_{\hat{j}}]_\ell \times \exp\{2\pi i(\hat{f}_d^k \cdot \frac{\lambda}{\lambda_{\hat{j}}} + \Delta f_{\hat{j}})t_\ell\}$ . Applying arrangement and phase correction, the estimated column of array matrix  $\mathbf{B} = \alpha \hat{\mathbf{A}}$  is obtained as:

$$\mathbf{b}_j = \alpha \hat{\mathbf{a}}_j = \hat{\rho}_k^* \cdot \hat{\xi}_k \quad (28)$$

For a general review, the total processing steps of the proposed detection algorithm is presented in Fig. 3.

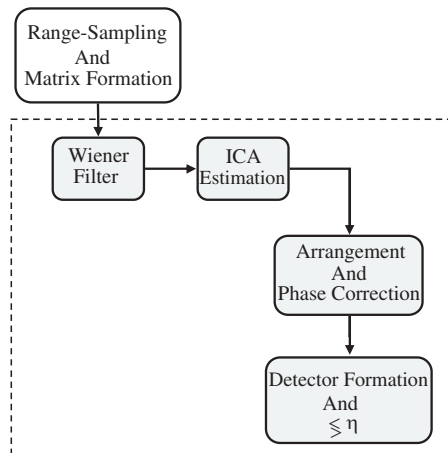


**Figure 3.** Block diagram of the presented ICA-based detector.

## 5. SIGNAL DESIGN

ICA is a powerful tool used to simplify our detection problem. In this paper, we use ICA estimation technique to separate the mixture of “the signal matrix” and “the array matrix”. In ICA techniques, information about mixed signals enables us to solve the estimation problem. Independency is the most important granted property, but other parameters about signals such as probability density function(PDF) should be considered too. Now the question is, which signals are better separated in this model? In other words, the performance of estimation with ICA should be evaluated by a quantitative parameter such as variance of error or in a more general case, Cramer Rao Bound (CRB). This question is the basis for designing the transmitted pulse trains.

As we completely described in [25] and as it was shown in [38, 39], the bounded magnitude signals such as BPSK and uniformly distributed signals have better performance according to the CRB. So, in this paper we consider them for radar signal design as described in the next subsection.

### 5.1. Code Sequence Design

In this paper, an ICA problem of the form demonstrated in Equation (10) is discussed. We can easily transform this time domain equation to an equivalent frequency domain by matrix multiplication as:

$$\mathbf{X}^f = \mathbf{X} \cdot \mathbf{F} = \mathbf{A}\tilde{\mathbf{S}} \cdot \mathbf{F} + \mathbf{N} \cdot \mathbf{F} = \mathbf{A}\tilde{\mathbf{S}}^f + \mathbf{N}^f \quad (29)$$

where  $\mathbf{F}$  is the  $L \times L$  matrix of discrete Fourier transform,  $\mathbf{X}^f$  is the  $m \times L$  matrix of the received signal in the frequency domain and  $\tilde{\mathbf{S}}^f$  contains the Fourier transform samples of  $\tilde{\mathbf{S}}$ . In the time domain, the frequency shift of the signal may affect the estimated values of the covariance matrix, higher order statistics and other statistical terms required in ICA estimation. Considering the doppler effect in the frequency domain, it can be seen that the effect may cause only a circular shift in the frequency samples of the signal. Therefore, the estimation of data statistics is more robust against the doppler variation in the frequency domain. Therefore, the frequency domain modeling of the signal as (29) leads to better results in ICA estimation. Solving this ICA problem, we will find the estimation of  $\mathbf{W} = (\alpha\mathbf{A})^{-1}$  named  $\hat{\mathbf{W}}$ .

In the frequency domain, doppler effect causes only a circular shift in the frequency samples, which does not change the statistical characteristics of the data. This forces us to apply our ICA estimator

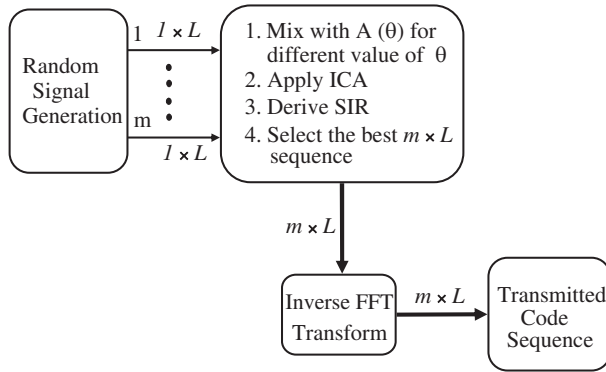


**Figure 4.** The structure used to select  $m$  batches of transmitted codes for the ICA-based estimator.

in the frequency domain. Therefore, the applied amplitude and phase code to the transmitted signal should be designed in a special manner to form a BPSK or uniformly distributed signal in the frequency domain. In this article, a computer search was used to select proper signals for the ICA technique. According to Fig. 4, different random BPSK or uniformly distributed signals are mixed by an array-matrix of some arbitrary directions and then an ICA estimator is applied to this mixture. The signal with the best separation performance according to [25], is selected as the frequency samples of the transmitted signal. In the next step, applying an inverse FFT to the samples, the  $m \times L$  code of the transmitted pulse train would be obtained.

## 6. ANALYSIS OF COMPUTATIONAL LOAD

In this section, a brief analysis of computational complexity of two presented detectors is offered. First, we should study the GLR detector of (14). According to [40], the straightforward method of  $n \times n$  matrix multiplication uses  $O(n^3)$  operations<sup>‡</sup>. It can be shown that the production of  $\mathbf{M}_{n \times p} \times \mathbf{Q}_{p \times \ell}$ , will result in complexity of  $O(np\ell)$ . Therefore, we can conclude that the order of complexity of (14) is:

$$O\left(n_f \times n_\theta \times n_\phi \times \left[2L \times (m^2 + 1) + m \times L^2\right]\right) \quad (30)$$

For the ICA-based detection algorithm presented in Fig. 3,

<sup>‡</sup>  $O(\cdot)$  (Big  $O$ ) notation is used in computer science to describe the performance or complexity of an algorithm.  $O(\cdot)$  specifically describes the worst-case scenario, and with a certain algorithm, it can be used to describe the execution time required or the space used (e.g., in memory or on disk).

different blocks should be considered independently. If we consider all possible values for  $L$ , the FFT block uses  $mL^2$  complex operations. Wiener filter has a complexity of  $O(m^2L + m^3)$  according to the structure described in Appendix C. For the JADE algorithm which is used as the ICA-estimator in this detection method, as described in [35, 36], the complexity is  $O((k + 2)m^3 + m^4 + 2m^2L)$ . Here  $k$  is the number of iterations in Approximate Joint Diagonalization (AJD) step in JADE algorithm as described in [41] and simulation results show that  $k$  does not exceed 20 in our detection problem. Also, the complexity of arrangement and phase estimation is  $O(n_f \times m^2L^2 + 4mL)$ . Finally, the complexity of (16) is  $O(n_\theta \times n_\phi \times m^3 + 2m^2L + mL^2)$ . Eventually, the order of complexity of the ICA-based detection algorithm is:

$$O(m^2L + km^3 + m^4 + n_f \times m^2L^2 + n_\theta \times n_\phi \times m^3) \quad (31)$$

It is important to note that in order to have an acceptable performance in both GLR and ICA-based detectors, the value of  $n_f$  should increase proportional to  $L$  and  $n_\phi$  should increase proportional to  $m$ . Comparison of (30) and (31) shows that because of the multiplicative form of parameters in (30), the computational load of GLR detector is much more than the ICA-based detector. For example, for a hypothetical system with parameters of  $m = 6$ ,  $n_f = 2L$ ,  $n_\phi = 2m$ ,  $n_\theta = 1000$  and  $k = 20$ , Fig. 5 compares the number of complex iterations for different values of  $L$  for both detectors. It can be easily seen that for these parameters, the difference of complexity between two detectors is of an order of  $10^3$ .

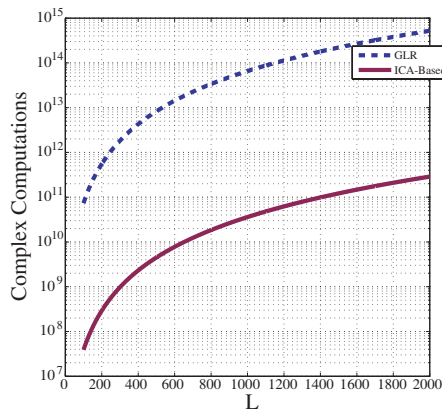


**Figure 5.** The number of complex computations versus  $L$ .

## 7. SIMULATION RESULTS

In this section, we consider a ULA array of omnidirectional transmit/receive antennas separated by  $0.5\lambda$ . As described in Section 2, in the system presented here, a small shift is applied to the frequency of different narrow-band transmitted signals. Considering a center frequency of  $f_c$  in these simulations,  $m$  transmitted frequencies are uniformly spaced in an interval of  $f_c \pm 5\%$ . In this section, an  $m = 6$  MIMO system with  $L = 200$  is considered and the obtained sequences according to Fig. 4 are used for simulation. Simulation results show that in order to have equivalent performance with the case of known  $\phi$  (Loss  $\leq 0.1$  dB), we should select  $n_\phi \geq 3m$ . So,  $n_\phi = 3m$  is used for the simulations in this section.

### 7.1. Sensitivity of Arrangement Algorithm to $n_f$

For the first simulation, sensitivity of the arrangement algorithm of Section 4.2.1 to  $n_f$  is discussed (this has been presented in [25], too). Hence, the probability of error (Pe) in the arrangement is derived for different numbers of frequency points ( $n_f$ ). Pe is calculated by averaging over all doppler values in the interval of  $[0, \text{PRF})$ . The result is shown in Fig. 6. It is shown that for ( $n_f > L/2$ ), the arrangement is ideally done for every doppler value of the received signal. In other words, the largest acceptable doppler step for proper arrangement is about  $2\text{PRF}/L$  ( $n_f = L/2$ ).

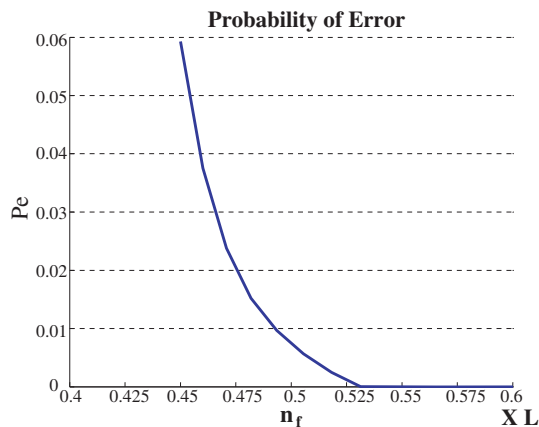


**Figure 6.** Probability of error in arrangement, for different frequency test points.

## 7.2. Code Selection

As mentioned in Section 5.1, a computer search is used to select proper transmitted signals for the ICA-based detector. The procedure is completely described in Fig. 4. In this procedure, different sets of uniformly distributed and random binary signals are applied. It is seen that ICA has a better performance in separation for the sets of uniformly distributed signals. So, in our simulations, this set of  $m \times L$  uniform signals (named *c1*) is utilized for ICA-based detector. A similar computer search is used for selecting a proper set of signals for GLR detector. In this procedure, different sets of uniform and random binary signals are studied. The set with the highest probability of detection ( $P_d$ ) is selected. It was found that the GLR detector is not so sensitive to the selected code. Therefore, in our simulations, a set of  $m \times L$  uniform signals named *c2* is utilized for the GLR detector.

## 7.3. Detection Performance

In this stage, the performance of the ICA-based and the GLR detectors for different SNR values of received signal is derived by simulation. In the following notation,  $P_{fa}$  denotes “probability of false alarm” and  $P_d$  denotes probability of detection for each detector. According to the results of Fig. 6, the number of frequency test point of arrangement algorithm of ICA-based detector is set to  $n_f = L/2$ . In order to check the doppler sensitivity of GLR detector, three different forms of this detector with  $n_f = L/2$ ,  $n_f = L$  and  $n_f > 2L$  are studied in this simulation. For the simulations of this section, a target with  $\theta = 20^\circ$  and  $\phi = 30^\circ$  is considered. The value of  $f_d$  for this target is adjusted to have the maximum frequency distance with the doppler test points. In Figs. 7 and 8, the power function of these four detectors is derived

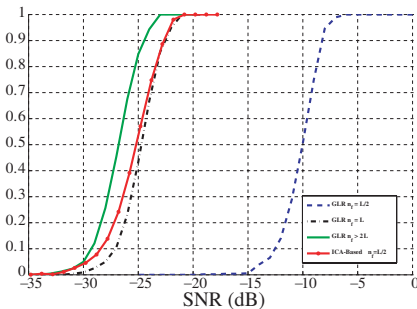


**Figure 7.** Power function of the GLR detector and the ICA-based detector for  $P_{fa} = 10^{-3}$ .

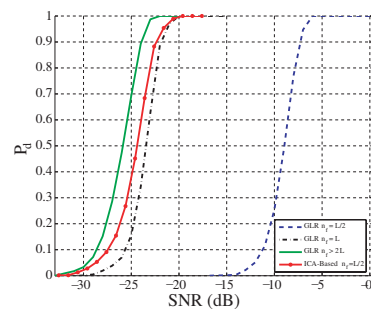


**Figure 8.** Power function of the GLR detector and the ICA-based detector for  $P_{fa} = 10^{-4}$ .

for  $P_{fa} = 10^{-3}$  and  $P_{fa} = 10^{-4}$ . It is shown that in identical condition of  $n_f = L/2$ , the GLR detector has a very poor detection performance compared to the ICA-based detector. Also, it can be seen that even with  $n_f = L$  the performance of the GLR detector is weaker than ICA-based detector with  $n_f = L/2$ . For example, for  $P_d = 0.9$  and  $P_{fa} = 10^{-3}$ , the GLR detector with  $n_f = L$  is about 0.2 dB weaker than ICA-based detector and this difference is even greater for lower values of  $P_d$ . This difference is about 0.4 dB for  $P_d = 0.9$  and  $P_{fa} = 10^{-4}$ . Figs. 7 and 8 show that unlike the ICA-based detector, the performance of the GLR detector is very sensitive to  $n_f$ . In this context, it is shown that changing  $n_f$  up to more than  $2L$  improves the performance of GLR detector about 2 dB.

## 8. CONCLUSION

The problem of target detection in a pulse-train co-located MIMO radar is investigated in this paper. Because of the unknown doppler value and unknown direction of target, we confront a compound hypothesis testing problem, so, a GLR detector is derived in this paper. As the complexity of the GLR detector is very high, the practical realization of this detector is very difficult. So, a new detector based on the theory of ICA algorithms is derived in this paper. In this context, a proper estimator is offered to rectify the phase and order ambiguity of ICA algorithms. A brief analysis of computational complexity of these two detectors is offered and it is shown that the computational load of the ICA-based detector is much less than the GLR detector. In addition, simulation results show that the sensitivity of the ICA-based detector to the doppler effect is very low. Thus, with equal number of doppler test points, better detection performance is gained in the ICA-based detector. Finally, an appropriate signal design method based on the separation performance of ICA algorithms is presented in this research.

## APPENDIX A. DERIVATION OF GLR DETECTOR

To solve the detection problem of (12), we should reform it to a vector structure of:

$$\mathbf{v}_x = \alpha \cdot \mathbf{H}(f_d) \cdot \mathbf{v}_A(\theta, \phi) + \mathbf{v}_N \quad (\text{A1})$$

where

$$\begin{aligned} \mathbf{v}_x &= \text{Vec}(\mathbf{X}^T) & \mathbf{v}_N &= \text{Vec}(\mathbf{N}^T) \\ \mathbf{v}_A(\theta, \phi) &= \text{Vec}(\mathbf{A}^T(\theta, \phi)) & \mathbf{H}(f_d) &= \mathbf{I}_m \otimes \tilde{\mathbf{S}}^T(f_d) \end{aligned} \quad (\text{A2})$$

In this equation  $\otimes$  denotes the Kronecker matrix product,  $\text{Vec}(\cdot)$  denotes the vectorization of a desired matrix and  $\mathbf{v}_N$  is the white gaussian noise vector that is  $\mathcal{N}(0, \sigma_n^2 \mathbf{I}_{L \times m})$ . Now, the detector of (13) can be formed as:

$$\max_{f_d, \alpha, \phi, \theta} \frac{f_{v_x}(\mathbf{v}_x | H_1, \theta, \alpha, \phi, f_d)}{f_{v_x}(\mathbf{v}_x | H_0)} \geq \eta \quad (\text{A3})$$

We can simplify (A3) by replacing the formulation of complex Gaussian PDFs as:

$$\max_{\alpha, f_d, \phi, \theta} \left\{ \frac{\exp \left[ -\frac{1}{\sigma^2} (\mathbf{v}_x - \alpha \cdot \mathbf{H}(f_d) \cdot \mathbf{v}_A(\theta, \phi))^H (\mathbf{v}_x - \alpha \cdot \mathbf{H}(f_d) \cdot \mathbf{v}_A(\theta, \phi)) \right]}{\exp \left[ -\frac{1}{\sigma^2} (\mathbf{v}_x)^H (\mathbf{v}_x) \right]} \right\} \geq \eta' \quad (\text{A4})$$

This equation can be simplified to:

$$\max_{f_d, \theta, \phi} \left\{ \max_{\alpha} \left\{ \text{Re} \left[ 2 \times \mathbf{v}_x^H \alpha \cdot \mathbf{H} \cdot \mathbf{v}_A - (\alpha \cdot \mathbf{H} \cdot \mathbf{v}_A)^H (\alpha \cdot \mathbf{H} \cdot \mathbf{v}_A) \right] \right\} \right\} \geq \eta \quad (\text{A5})$$

The maximization over  $\alpha$  is derived by applying a derivative to inner argument of  $\text{Re}[\cdot]$  in (A5) and we have:

$$\begin{aligned} 2 \times \mathbf{v}_x^H \cdot \mathbf{H} \cdot \mathbf{v}_A - 2 \times \alpha^* (\mathbf{H} \cdot \mathbf{v}_A)^H (\mathbf{H} \cdot \mathbf{v}_A) &= 0 \quad (\text{A6}) \\ \Rightarrow \hat{\alpha} &= \frac{(\mathbf{H} \cdot \mathbf{v}_A)^H \mathbf{v}_x}{(\mathbf{H} \cdot \mathbf{v}_A)^H (\mathbf{H} \cdot \mathbf{v}_A)} \end{aligned}$$

Replacing  $\hat{\alpha}$  in (A5), the detector can be simplified to:

$$\max_{f_d, \theta, \phi} \frac{\mathbf{v}_x^H (\mathbf{H} \mathbf{v}_A) (\mathbf{H} \mathbf{v}_A)^H \mathbf{v}_x}{(\mathbf{H} \mathbf{v}_A)^H (\mathbf{H} \mathbf{v}_A)} \geq \eta \quad (\text{A7})$$

According to (A2) we have:

$$\mathbf{H} \mathbf{v}_A = \left( \mathbf{I}_m \otimes \tilde{\mathbf{S}}^T \right) \text{Vec}(\mathbf{A}^T) = \text{Vec}(\tilde{\mathbf{S}}^T \mathbf{A}^T) \quad (\text{A8})$$

and then

$$(\mathbf{H} \mathbf{v}_A)^H (\mathbf{H} \mathbf{v}_A) = \left\| \tilde{\mathbf{S}}^T \mathbf{A}^T \right\|^2 = \left\| \mathbf{A} \tilde{\mathbf{S}} \right\|^2 \quad (\text{A9})$$

Also according to (A2) we have:

$$(\mathbf{H} \mathbf{v}_A)^H \mathbf{v}_x = \text{Vec}(\tilde{\mathbf{S}}^T \mathbf{A}^T)^H \text{Vec}(\mathbf{X}^T) = \left( \text{tr}(\mathbf{A} \tilde{\mathbf{S}} \mathbf{X}^H) \right)^* \quad (\text{A10})$$

Replacing (A9) and (A10) in (A7), the GLR detector is:

$$\max_{f_d, \theta, \phi} \frac{\left| \text{tr}(\mathbf{A}(\theta, \phi) \tilde{\mathbf{S}}(f_d) \mathbf{X}^H) \right|^2}{\left\| \mathbf{A}(\theta, \phi) \tilde{\mathbf{S}}(f_d) \right\|^2} \geq \eta \quad (\text{A11})$$

### APPENDIX B. DERIVATION OF ICA-BASED DETECTOR

To derive an ICA-based detector for (12), we should initially reform it to a vector structure as:

$$\mathbf{v}_x = \alpha \cdot \mathbf{H}(f_d) \cdot \mathbf{v}_A(\theta, \phi) + \mathbf{v}_N \tag{B1}$$

where the same definitions as (A2) are true in this notation too. In this equation,  $\mathbf{v}_N$  is the white Gaussian noise vector of  $\mathcal{N}(0, \sigma_n^2 \mathbf{I}_{L \times m})$ . Now, the detector of (15) can be formed as:

$$\frac{f_{v_x}(\mathbf{v}_x | H_1, \check{\theta}, \check{\alpha}, \check{\phi}, \check{f}_d)}{f_{v_x}(\mathbf{v}_x | H_0)} \geq \eta \tag{B2}$$

where  $\check{\theta}$ ,  $\check{\alpha}$ ,  $\check{\phi}$  and  $\check{f}_d$  are the ICA estimations of  $\theta$ ,  $\alpha$ ,  $\phi$  and  $f_d$ . We can simplify (B2) by replacing the formulation of complex Gaussian PDFs as:

$$\frac{\exp\left[-\frac{1}{\sigma^2} (\mathbf{v}_x - \check{\alpha} \cdot \mathbf{H}(\check{f}_d) \cdot \mathbf{v}_A(\check{\theta}, \check{\phi}))^H (\mathbf{v}_x - \check{\alpha} \cdot \mathbf{H}(\check{f}_d) \cdot \mathbf{v}_A(\check{\theta}, \check{\phi}))\right]}{\exp\left[-\frac{1}{\sigma^2} (\mathbf{v}_x)^H (\mathbf{v}_x)\right]} \geq \eta' \tag{B3}$$

This equation can be simplified to:

$$\begin{aligned} & \text{Re}\left[2 \times \mathbf{v}_x^H \check{\alpha} \cdot \mathbf{H}(\check{f}_d) \cdot \mathbf{v}_A(\check{\theta}, \check{\phi}) - (\check{\alpha} \cdot \mathbf{H}(\check{f}_d) \cdot \mathbf{v}_A(\check{\theta}, \check{\phi}))^H \right. \\ & \left. (\check{\alpha} \cdot \mathbf{H}(\check{f}_d) \cdot \mathbf{v}_A(\check{\theta}, \check{\phi}))\right] \geq \eta \end{aligned} \tag{B4}$$

According to (A2) the ICA-based detector is:

$$\left|2\text{Re}\left[\text{tr}\left(\check{\alpha} \mathbf{A}(\check{\theta}, \check{\phi}) \tilde{\mathbf{S}}(\check{f}_d) \mathbf{X}^H\right)\right] - \left\|\check{\alpha} \mathbf{A}(\check{\theta}, \check{\phi}) \tilde{\mathbf{S}}(\check{f}_d)\right\|^2\right| \geq \eta \tag{B5}$$

### APPENDIX C. WIENER FILTER

Considering the described model in Section 2, the received signal of (10) is composed of  $L$  independent samples (pulses) of  $m \times 1$  receiver vector. For each pulse, the vector of  $m$  received signals can be formulated as

$$\mathbf{x} = \mathbf{A}\tilde{\mathbf{s}} + \mathbf{n} = \mathbf{q} + \mathbf{n} \tag{C1}$$

where  $\mathbf{n}$  is the vector of i.i.d. noise variables. Considering a white Gaussian distribution as  $\mathcal{N}(0, \sigma_n^2)$ , we can form the Wiener filter [42] or equivalently Linear Mean Square estimator of  $\mathbf{q}$  as

$$\mathbf{F} = \mathbf{R}_x^{-1} \mathbf{R}_{qx} \tag{C2}$$

where  $\mathbf{R}_x$  is the correlation matrix of received data and  $\mathbf{R}_{qx}$  is the cross-correlation matrix of data and signal. By definition we have

$$\begin{aligned}\mathbf{R}_x &= E \{ \mathbf{x}\mathbf{x}^H \} \\ \mathbf{R}_{qx} &= E \{ \mathbf{q}\mathbf{x}^H \} = E \{ \mathbf{q}\mathbf{q}^H \} = \mathbf{R}_q\end{aligned}\tag{C3}$$

But as only  $L$  samples of each variable is available in this model, the estimated form of these parameters are

$$\begin{aligned}\hat{\mathbf{R}}_x &= \mathbf{X}\mathbf{X}^H/L \\ \hat{\mathbf{R}}_q &= \mathbf{X}\mathbf{X}^H/L - \sigma_n^2 \mathbf{I}_{m \times m}\end{aligned}\tag{C4}$$

By applying  $\hat{\mathbf{F}} = \hat{\mathbf{R}}_x^{-1} \hat{\mathbf{R}}_q$  as a pre-multiply operation to the signal matrix, we have

$$\tilde{\mathbf{X}} = \hat{\mathbf{F}}\mathbf{X} = \mathbf{A}\tilde{\mathbf{S}} + \mathbf{E}\tag{C5}$$

where  $\mathbf{E} = \tilde{\mathbf{X}} - \mathbf{A}\tilde{\mathbf{S}}$  is the error of estimation.

## REFERENCES

1. Skolnik, M. I., *Introduction to Radar Systems*, 3rd edition, McGraw-Hill, New York, 2001.
2. Haykin, S., J. Litva, and T. J. Shepherd, *Radar Array Processing*, Springer-Verlag, New York, 1993.
3. Fishler, E., A. Haimovich, R. Blum, D. Chizhik, L. Cimini, and R. Valenzuela, "MIMO radar: An idea whose time has come," *Proc. of the IEEE Radar Conf.*, Vol. 2, 71–78, Honolulu, Hawaii, Apr. 2004.
4. Haimovich, A., R. Blum, and L. Cimini, "MIMO radar with widely separated antennas," *IEEE Signal Process. Mag.*, Vol. 25, 116–129, Jan. 2008.
5. Fishler, E., A. Haimovich, R. Blum, L. Cimini, D. Chizhik, and R. Valenzuela, "Spatial diversity in radars-models and detection performance," *IEEE Transactions on Signal Processing*, Vol. 54, 823–838, Mar. 2006.
6. Lehmann, N., E. Fishler, A. Haimovich, R. Blum, D. Chizhik, L. Cimini, and R. Valenzuela, "Evaluation of transmit diversity in MIMO radar direction finding," *IEEE Transactions on Signal Processing*, Vol. 55, 2215–2225, May 2007.
7. Li, J., P. Stoica, and X. Zheng, "Signal synthesis and receiver design for MIMO radar imaging," *IEEE Transactions on Signal Processing*, Vol. 56, 3959–3968, Aug. 2008.
8. Li, J. and P. Stoica, "MIMO radar with colocated antennas," *IEEE Signal Process. Mag.*, Vol. 24, 106114, Sep. 2007.

9. Chen, C. Y. and P. Vaidyanathan, "MIMO radar space-time adaptive processing using prolate spheroidal wave functions," *IEEE Transactions on Signal Processing*, Vol. 56, 106–114, Sep. 2007.
10. Bekkerman, I. and J. Tabrikian, "Target detection and localization using MIMO radars and sonars," *IEEE Transactions on Signal Processing*, Vol. 54, 3873–3883, Oct. 2006.
11. Daum, F. and J. Huang, "MIMO radar: Snake oil or good idea," *IEEE Aerosp. Electron. Syst. Mag.*, 8–12, May 2009.
12. Sheikhi, A. and A. Zamani, "Temporal coherent adaptive target detection for multi-input multi-output radars in clutter," *IET Radar, Sonar & Navig.*, Vol. 2, 86–96, Jun. 2008.
13. De Maio, A. and M. Lops, "Design principles of MIMO radar detectors," *IEEE Transactions on Aerospace and Electronic Systems*, Vol. 43, 886–897, Jul. 2007.
14. Huang, Y., P. Brennan, D. Patrick, I. Weller, P. Roberts, and K. Hughes, "FMCW based MIMO imaging radar for maritime navigation," *Progress In Electromagnetics Research*, Vol. 115, 327–342, 2011.
15. Chen, J., Z. Li, and C. Li, "A novel strategy for topside ionosphere sounder based on spaceborne MIMO radar with fdcd," *Progress In Electromagnetics Research*, Vol. 116, 381–393, 2011.
16. Lim, S.-H., C. G. Hwang, S.-Y. Kim, and N.-H. Myung, "Shifting MIMO SAR system for high-resolution wide-swath imaging," *Journal of Electromagnetic Waves and Applications*, Vol. 25, No. 8–9, 1168–1178, 2011.
17. Yang, Y. and R. S. Blum, "Minimax robust MIMO radar waveform design," *IEEE Journal of Sel. Topics Signal Process.*, Vol. 1, 147–155, 2007.
18. Fuhrmann, D. and G. Antonio, "Transmit beamforming for MIMO radar systems using signal cross-correlation," *IEEE Trans. on Aerospace and Electronic Systems*, Vol. 44, 171–176, Jan. 2008.
19. Qu, Y., G. Liao, S.-Q. Zhu, X.-Y. Liu, and H. Jiang, "Performance analysis of beamforming for MIMO radar," *Progress In Electromagnetics Research*, Vol. 84 123–134, 2008.
20. Sinha, N. B., R. N. Bera, and M. Mitra, "Digital array MIMO radar and its performance analysis," *Progress In Electromagnetics Research C*, Vol. 4, 25–41, 2008.
21. Hassanien, A. and S. A. Vorobyov, "Phased-MIMO radar: A tradeoff between phased-array and MIMO radars," *IEEE Transactions on Signal Processing*, Vol. 58, 3137–3151, Jun. 2010.

22. Zhang, J., H. Wang, and X. Zhu, "Adaptive waveform design for separated transmit/receive ULA-MIMO radar," *IEEE Transactions on Signal Processing*, Vol. 58, 4936–4942, Sep. 2010.
23. Sen, S. and A. Nehorai, "OFDM MIMO radar with mutual-information waveform design for low-grazing angle tracking," *IEEE Transactions on Signal Processing*, Vol. 58, 3152–3162, Jun. 2010.
24. Li, H. and B. Himed, "Transmit subaperturing for MIMO radars with co-located antennas," *IEEE Journal of Selected Topics in Signal Processing*, Vol. 4, 55–65, Feb. 2010.
25. Hatam, M., A. Sheikhi, and M. A. Masnadi-Shirazi, "A pulse-train mimo radar based on theory of independent component analysis," *Submitted for Publication in the Iranian Journal of Science and Technology*, Jun. 2011.
26. Cui, G., L. Kong, and X. Yang, "Multiple-input multiple-output radar detectors design in non-gaussian clutter," *IET Radar, Sonar & Navig.*, Vol. 4, 724–732, 2010.
27. Levenon, N., "Stepped-frequency pulse-train radar signal," *IEE Proc. of Radar, Sonar and Navigation*, Vol. 149, 297–309, Dec. 2002.
28. Iizuka, K., A. P. Freundorfer, et al., "Step-frequency radar," *Journal of Applied physics*, Vol. 56, 2572–2583, Nov. 1984.
29. Mohseni, R., A. Sheikhi, and M. A. Masnadi-Shirazi, "Compression of multicarrier phase-coded radar signals based on discrete fourier transform (DFT)," *Progress In Electromagnetics Research C*, Vol. 5, 93–117, 2008.
30. Gabriel, J. R. and S. M. Kay, "On the relationship between the GLRT and UMPI tests for the detection of signals with unknown parameters," *IEEE Transactions on Signal Processing*, Vol. 53, 4194–4203, Nov. 2005.
31. Hyvärinen, A., J. Karhunen, and E. Oja, *Independent Component Analysis*, John Wiley and Sons, New York, 2001.
32. Comon, P., "Independent components analysis: A new concept?," *Special Issue on Higher-order Statistics, Signal Processing, Elsevier*, Vol. 36, 287–314, Apr. 1994.
33. Belouchrani, A., K. A. Meraim, J. F. Cardoso, and E. Moulines, "A blind source separation technique based on second order statistics," *IEEE Transactions on Signal Process*, Vol. 45, 434–444, 1997.
34. Hyvärinen, A. and E. Oja, "A fast fixed-point algorithm for independent component analysis," *IEEE Transactions on Neural*

- Computations*, Vol. 9, 1483–1492, Oct. 1997.
35. Cardoso, J. F. and A. Souloumiac, “Blind beamforming for non gaussian signals,” *IEE Proceedings F, Radar and Signal Processing*, Vol. 140, 362–370, Dec. 1993.
  36. Cardoso, J. F., “Jade algorithm for complex-valued signals as a matlab function,” <http://perso.telecom-paristech.fr/~cardoso/Algo/Jade/jade.m>.
  37. Kay, S. M., *Fundamentals of Statistical Signal Processing: Estimation Theory*, Vol. 1, Prentice-Hall, 1998.
  38. Tichavský, P., Z. Koldovský, and E. Oja, “Performance analysis of the FastICA algorithm and Cramer-Rao bounds for linear independent component analysis,” *IEEE Transactions on Signal Processing*, Vol. 54, 1189–1203, Apr. 2006.
  39. Koldovský, Z., P. Tichavský, and E. Oja, “Efficient variant of algorithm FastICA for independent component analysis attaining the Cramr-Rao lower bound,” *IEEE Transactions on Neural Networks*, Vol. 17, 806–815, Sep. 2006.
  40. Holtz, O. and N. Shomron, “Computational complexity and numerical stability of linear problems,” *Proceedings of the 5th European Congress of Mathematics*, 381–400, EMS Publishing House, 2010.
  41. Todros, K. and J. Tabrikian, “Fast approximate joint diagonalization of positive definite hermitian matrices,” *IEEE International Conference on Acoustics, Speech and Signal Processing*, Vol. 3, 2007.
  42. Papoulis, A. and S. Pillai, *Probability, Random Variables and Stochastic Processes*, 4th edition, Mc-Graw-Hill, 2002.